



Ferulic acid attenuates oxidative DNA damage and inflammatory responses in microglia induced by benzo(a)pyrene



Yongfen Bao^{a,1}, Qingjie Chen^{b,1}, Yushuang Xie^c, Zhe Tao^c, Kehua Jin^a, Shuli Chen^a, Yuting Bai^{d,*}, Jun Yang^{e,f,*}, Shigang Shan^{a,*}

^a Research Center of Basic Medical Sciences, School of Basic Medical Sciences, Hubei University of Science and Technology, Xianning 437100, China

^b Hubei Key Laboratory of Genetics and Molecular Mechanisms of Cardiological Disorders, Hubei University of Science and Technology, Xianning 437000, China

^c School of Pharmacy, Hubei University of Science and Technology, Xianning 437100, China

^d School of Clinical Medicine, Hubei University of Science and Technology, Xianning 437100, China

^e Department of Public Health, Hangzhou Normal University School of Medicine, 16 Xuelin Street, Hangzhou 310016, China

^f Zhejiang Provincial Center for Uterine Cancer Diagnosis and Therapy Research, The Affiliated Women's Hospital, Zhejiang University, 1 Xueshi Road, Hangzhou 310003, China

ARTICLE INFO

Keywords:

Ferulic acid
Microglial cells
Benzo(a)pyrene
Inflammasome
DNA damage
NOD-like receptor (NLR) family pyrin domain-containing 3

ABSTRACT

Over-activation of microglia disrupts the physiological homeostasis of the brain, and induces inflammatory response and other processes which are implicated in neurodegenerative diseases. Therefore, theoretically, suppression of neuroinflammation would slow the progression of neurodegenerative disease. In this study, we investigated the possible protective effects of Ferulic acid (FA) against benzo(a)pyrene (BaP)-induced microglial activation using BV2 cells as the model system. Exposure of BV2 cells to BaP (10 μ M) significantly increased DNA damage and the production of pro-inflammatory mediators, including nitric oxide (NO), inducible nitric oxide synthase (iNOS), cyclooxygenase-2 (COX-2), reactive oxygen species (ROS), malondialdehyde (MDA), and cytokines (interleukins-1 β and -6). On the other hand, when BaP-treated BV2 cells were further incubated with FA (10, 20, 40, or 80 mg/mL) for another 24 h, a significant reduction in BaP-induced DNA damage and the release of multiple pro-inflammatory and cytotoxic factors (including interleukin-1 β , interleukin-6, NO, and ROS) was observed in a dose-dependent manner. Further study revealed that the microglial NOD-like receptor (NLR) family pyrin domain-containing 3 (NLRP3) signaling pathway was involved in the protective effect of FA. Taken together, these results suggested that FA suppressed BaP-induced toxicity in microglia, and thus may exert neuroprotective effects by inhibiting microglia-mediated pro-inflammatory response.

1. Introduction

Neuroinflammation is termed as the chronic inflammation within the brain, which can lead to certain neurodegenerative events such as dystrophic neuronal growth. One of the characteristics associated with neuroinflammation is the activation of glial cells, most notably microglial cells. Microglial cells, the resident macrophage cells of the central nervous system (CNS), play pivotal roles in innate immune regulation and neuronal homeostasis. It has been shown that microglial cells grow larger and assume an ameboid shape upon activation, which in turn up-

regulate the production of various neurotoxic pro-inflammation mediators, including cytokines, chemokines, and prostaglandins [1,2]. The generated pro-inflammatory cytokines then can directly affect the CNS, eventually leading to functional alteration of the brain and behavioral changes [3–5]. For instance, it has been reported that neuroinflammation induced by the activation of glial cells can cause neuronal death and impair memory [6–8], while the overproduction of inflammatory cytokines is implicated in the progression of neurodegenerative diseases such as Alzheimer's disease and Parkinson's disease [9].

Many factors can lead to inflammation in the CNS, including tissue

Abbreviations: FA, ferulic acid; NLRP3, NOD-like receptor (NLR) family pyrin domain-containing 3; ROS, reactive oxygen species; NO, nitric oxide; IL-1 β , interleukins-1 β ; IL-6, interleukins-6; BaP, benzo[a]pyrene; APDC, 4-amino-2,4-pyrrolidine-dicarboxylic acid; MDA, malondialdehyde

* Corresponding authors at: School of Clinical Medicine, Hubei University of Science and Technology, Xianning 437100, China (Y. Bai). Department of Public Health, Hangzhou Normal University School of Medicine, 16 Xuelin Street, Hangzhou 310016, China (J. Yang). Research Center of Basic Medical Sciences, School of Basic Medical Sciences, Hubei University of Science and Technology, Xianning 437100, China (S. Shan).

E-mail addresses: 345446098@qq.com (Y. Bai), gastate@zju.edu.cn (J. Yang), ssgang121@163.com (S. Shan).

¹ These authors contributed equally to this work.

<https://doi.org/10.1016/j.intimp.2019.105980>

Received 14 August 2019; Received in revised form 1 October 2019; Accepted 13 October 2019

Available online 04 November 2019

1567-5769/ © 2019 Elsevier B.V. All rights reserved.

damage, trauma, infection, and exposure to environmental toxic agents such as Benzo(a)pyrene (BaP). BaP is a well-studied member of the polycyclic aromatic hydrocarbon (PAH) family, and a well-known Group 1 carcinogen classified by the International Agency for Research on Cancer (IARC) [10]. As a lipophilic compound, BaP can easily cross the blood–brain barrier (BBB) and thereby gaining direct access to the CNS [11–13]. Indeed, exposure to BaP had been reported to induce behavioral deficits in rat and human, indicating the neurotoxicity of BaP [14–17]. Further mechanistic study revealed that BaP-induced pro-inflammatory cytokines, including tumor necrosis factor- α (TNF- α), interleukin-1 β (IL-1 β), IL-6, etc., are involved in these events [18–20]. Interestingly, BaP can act synergistically with TNF- α to further aggravate the inflammatory responses, including the generation/activation of the inducible isoforms of NO synthase (iNOS), cyclooxygenase-2 (COX-2), prostaglandin E2 (PGE2), as well as IL-6 and the p38 kinase [21].

BaP can be metabolized to form reactive intermediates such as BaP-quinones, which can lead to the generation of reactive oxygen species (ROS) and are associated with the oxidative alteration of DNA, proteins, and anti-oxidant enzymes [22,23]. It is also well documented that excessive expression of iNOS is associated with chronic inflammatory diseases by promoting NO production [24,25]. Similarly, COX-2 is another well-documented important proinflammatory mediator, which is involved in PGE2 generation and eventually resulted in neurodegenerative diseases [26]. Such claim has been supported by recent studies that neurotoxicity could be enhanced by excessive production of COX-2-mediated PGE2 from microglia; furthermore, a selective COX-2 inhibitor, celecoxib, can significantly reduce systemic brain inflammation and white matter injury in neonatal rats, and the underlying mechanism is contributed to the suppression of PGE2 production [27,28]. Based on these observations, it is proposed that the attenuation of proinflammatory mediators such as NO and PGE2, as well as the expression of their representative genes such as iNOS and COX-2 in microglial cells, could be an important therapeutic strategy for the prevention of neuronal inflammation and the pathological consequences.

IL-1 β is regarded as one of the most important pro-inflammatory cytokines, and the multiprotein complex NOD-like receptor (NLR) family pyrin domain-containing 3 (NLRP3) inflammasome is responsible for the release of IL-1 β and IL-18 from innate cells. NLRP3 recruits and activates caspase-1 through the adaptor protein ASC (apoptosis-associated speck like protein containing a CARD domain), leading to the cleavage and activation of IL-1 β and IL-18 precursors. Many factors can activate the NLRP3 inflammasome, including whole live bacteria, fungal and viral pathogens, as well as various pathogen-associated molecular patterns (PAMPs) and damage-associated molecular patterns (DAMPs) [29]. In addition, NLRP3 inflammasome can also be active by cellular stress triggered by factors such as oxidative stress or lysosomal damage [30], and ROS generation had been proposed as a crucial step for the activation process [9].

As stated above, it is clear that the reduction/inhibition of inflammatory mediators could attenuate the severity of neurodegenerative diseases [5], thus the suppression of microglial activation and subsequent down-regulation of neurotoxic pro-inflammatory mediators would be a useful therapeutic approach. Ferulic acid (FA) is an important component of many widely used medicinal herbs, which belongs to the family of hydroxycinnamic acid. It has structural resemblance to curcumin, and the pure form of FA is a yellowish powder (Fig. 1). FA can be found in high abundance in the leaves and seeds of many plants, especially in cereals made from brown rice, whole wheat, and oats. Many studies have shown that FA has valuable pharmacological properties such as neuronal progenitor cell proliferation, anti-inflammatory, antioxidant, and neuroprotective activities [31–35]. In particular, the neuroprotective effect of FA has been reported in many studies including brain injury, spinal ischemia, and Alzheimer-like pathology [36–38]. Nonetheless, the underlying molecular mechanisms are still not fully understood.

Therefore, in the present study, we intended to determine whether the anti-inflammatory effect of FA contributed to its protective effect. As reported here, while BaP could induce oxidative stress and DNA damage, as well as the expression of many factors involved in pro-inflammatory response in microglia BV2 cells, FA protected BV2 from BaP-induced DNA damage and suppressed the pro-inflammatory response. Further detailed study revealed that the possible anti-inflammatory mechanisms of FA might involve the NLRP3 pathway in microglial cells.

2. Materials and methods

2.1. Reagents and antibodies

Hanks Balanced Salt Solution, (4-(2-hydroxyethyl)-1-piperazineethanesulfonic acid) (HEPES), ethanol, dimethyl sulfoxide (DMSO), benzo(a)pyrene (BaP), and 96 well plates were all purchased from Sigma-Aldrich Co. (St. Louis, MO). Dulbecco's Eagle's Medium (DMEM), fetal bovine serum (FBS), penicillin, streptomycin, and trypsin/EDTA were purchased from Hyclone (Logan, UT). ELISA Set of IL-1 β , IL-6, and a 3,3',5,5'-Tetramethylbenzidine (TMB) Substrate Reagent Set were purchased from BD Biosciences (Franklin Lakes, SD). Antibodies against iNOS, COX-2, Pro-IL-1 β , IL-1 β , caspase-1, Pro-caspase-1, and NLRP3 were purchased from Santa Cruz Biotechnology (Santa Cruz, CA). Antibody against β -actin and the secondary antibodies were obtained from Bioworld Technology (Nanjing, China). RNeasy Mini extraction kit, RT² first Strand Kit, SYBR Green Fluor PCR Mastermix were purchased from Qiagen (Manchester, UK), PCR primers were synthesized at GenePharma (Shanghai, China). Malondialdehyde (MDA) assay kit and the total nitrate assay kit were obtained from Beyotime (Shanghai, China). All other chemicals used were of analytical grade.

2.2. Cell culture and treatment

BV2 cells were obtained from the American Type Culture Collection (ATCC, Manassas, VA) and maintained in DMEM supplemented with 10% heat-inactivated FBS and 100 μ M of 2-Mercaptoethanol. BV-2 cells were cultured and treated as described earlier [39]. Briefly, cells were seeded at the density of 5×10^4 cells/ml, pretreated for 1 h with 10 μ M BaP before incubation in medium containing various concentrations of FA (2.5, 5, 10, 20, 40, and 80 mg/mL). For cell treatments, a stock solution of FA was prepared freshly prior to use, with dimethylsulfoxide (DMSO) as the solvent, and the final concentration of DMSO in the incubation mixture never exceeded 0.1%.

2.3. Determination of cell viability

Cell viability was analyzed using a Cell Counting Kit-8 according to the manufacturer's instructions (Dojindo Kumamoto, Japan). Briefly, 1×10^4 cells were inoculated into 96-well plates, then treated with BaP (0.01–50 μ M) or FA (2.5, 5, 10, 20, 40, and 80 mg/mL) for 24 h. To evaluate the effects of FA on BaP-treated cells, cells were first treated with BaP for 1 h, then FA was added to cells (with BaP still in the medium) and incubated for another 24 h. After various treatments, 90 μ l of medium and 10 μ l of CCK-8 solution were added to each well. The cells were then incubated at 37 $^{\circ}$ C for 2 h. After incubation, the absorption at 450 nm was measured using an Infinite M200 Microplate Reader (Tecan, Switzerland). Cell viability was calculated as the absorbance of treated cell/control \times 100%.

2.4. Alkaline comet assay and quantification of DNA damage

The alkaline comet assay was conducted as described by Yu et al. [40]. A 24-h time course was first conducted to determine the best observation time for the different treatments. In short, after FA or BaP

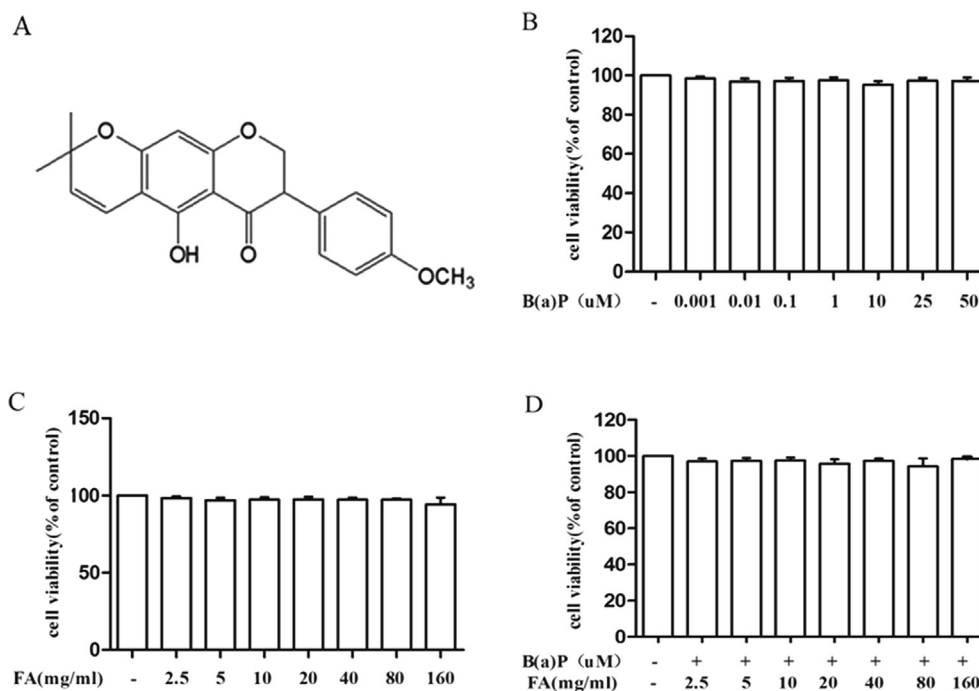


Fig. 1. FA and BaP do not affect BV2 cell viability. (A) Structure of FA. After BV2 cells were treated with BaP (0.01–50 μM) (B), or FA (2.5, 5, 10, 20, 40, 80, 160 mg/ml) (C), or treated with BaP (10 μM L⁻¹) for 1 h followed by FA treatment (D) for 24 h, cell viability was determined by CCK-8 assay.

treatment, BV2 cells were trypsinized and centrifuged. Then cell pellets were mixed with 70 μl of 0.7% low melting point agarose at 37 $^{\circ}\text{C}$ and placed on microscope slides pre-coated with a thin layer of 0.5% normal melting agarose. After cooling at 4 $^{\circ}\text{C}$ for 5 min, slides were covered with another layer of low-melting agarose. After solidification at 4 $^{\circ}\text{C}$ for 5 min, slides were immersed in a cold, freshly prepared lysing solution for 60 min. After that, the slides were removed and placed close together in a horizontal gel electrophoresis tank filled with fresh alkaline buffer (1 mM disodium EDTA and 300 mM NaOH, pH13) for 20 min at 4 $^{\circ}\text{C}$. Electrophoresis was conducted at 4 $^{\circ}\text{C}$ at 25 V and 300 mA for 20 min. Then the slides were washed in distilled water, and Tris buffer (0.4 M Tris, pH 7.5) was added to neutralize excess alkali. After washing, the slides were allowed to dry at room temperature prior to staining with ethidium bromide. The whole procedure was carried out in dim light to prevent additional DNA damage. Fifty cells of each sample (25 from each end of the slide) were randomly picked and analyzed using Komet 4.0.2 imaging software (Kinetic Imaging Ltd, Liverpool, UK). The Olive tail moment was calculated as [(tail mean-head mean) \times (tail % DNA/100)] and used as the parameter for measuring DNA damage.

2.5. NO assay

NO production by BV2 cells was determined using Griess reagent kit (Invitrogen, Frederick, MD). Briefly, Griess reagent was prepared by mixing equal amounts of sulfanilic acid and N-(1-naphthyl) ethylenediamine. After 30 min incubation with samples, absorbance was read at 540 nm using a microplate reader.

2.6. Measurement of intracellular ROS generation

Production of intracellular reactive oxygen species (ROS) in BV2 cells was determined based on the oxidation of DCFH-DA (S0033, Beyotime Company, Shanghai, China). Fluorescence emission at 525 nm following excitation at 488 nm was measured using a microplate reader. The cellular fluorescence intensity was expressed as the fold change relative to the level observed in the control cells.

2.7. Determination of MDA levels

Lipid peroxidation MDA assay kit (Beyotime, Nantong, China) was used to measure the MDA level according to the manufacturer's instructions. Cells were lysed with lysis buffer (1:10) (Beyotime, Nantong, China) on the ice and centrifuged at 1600 rpm for 10 min for the supernatant. BCA Protein Assay Kit (Pierce Biotechnology, USA) was used to measure the protein concentrations. TBA storage solution and TBA dilution were prepared to make MDA working solution. Then, MDA level was detected.

2.8. Immunoblot analysis

Total cellular extracts were prepared by lysing cells in ice-cold RIPA buffer (10 mM Tris-Cl (pH 7.4), 150 mM NaCl, 1% Triton X-100, 1% deoxycholate, 0.1% SDS, 355 mM EDTA, protease inhibitor cocktail (Complete Mini protease inhibitor cocktail, Roche), phosphatase inhibitor cocktail (PhosStop, Roche), 1 mM β -mercaptoethanol. Equivalent protein extracts (40–60 μg) were denatured by boiling in SDS and β -mercaptoethanol before being separated by SDS-PAGE and transferred onto PVDF membranes (Bio-Rad Laboratories). The blots were blocked with 5% nonfat dry milk in TBS-0.1% Tween20 (TBS-T), and incubated overnight at 4 $^{\circ}\text{C}$ with respective primary antibodies (1:1000 dilution). Membranes were then washed with TBS-T and incubated with secondary IRDye 680LT Goat anti-rabbit or IRDye 680LT Goat anti-mouse (1:20,000) at room temperature for 1 h. Bands were visualized using the Li-Cor Odyssey Infrared Imaging System (Li-Cor, USA). Immunoblots shown in the figures are representative images of at least three independent experiments.

2.9. Quantitative real-time polymerase chain reaction (qRT-PCR)

For qRT-PCR, BV2 cells were seeded in six-well culture plates (5×10^5 /well) and cultured overnight. After various treatments, total RNA was isolated using RNeasy Mini extraction kit (Qiagen, Cat# 74104) and then first-strand cDNA was synthesized using RT² first Strand Kit (Qiagen, Cat.# 330401) following the manufacturer's

protocol. PCR amplification was performed using RT² SYBR Green Fluor PCR Mastermix (Qiagen, Cat.# 330510). Amplification was performed using an Applied Biosystems 7500 Real-Time PCR System. Oligonucleotide primers are: β -actin (F 5'-CGT GAC ATT AAG GAG AAG CTG-3'; R 5'-CTA GAA GCA TTT GCG GTG GAC-3'); NLRP3 (F 5'-CTT CCT TTC CAG TTT GCT GC-3'; R 5'-TAT CTC CAT TGC CAT TCA-3'). From each sample 25 μ l PCR product was used to run the RT² Profiler PCR array (Qiagen, PAMM-150A-2) according to the manufacturer's protocol. The PCR thermal cycling programs were: denaturation at 95 °C for 10 min, followed by 40 cycles at 95 °C for 15 s, 60 °C for 1 min. Data analysis was performed using RT² Profiler PCR array data analysis on line software (<http://www.sabiosciences.com/pcrarraydataanalysis.php>).

2.10. Measurement of IL-1 β and IL-6

The Enzyme-Linked ImmunoSorbent Assay (BD, Franklin Lakes, SD) kits were used to quantify cytokine levels in BV-2 cell culture supernatants. BV-2 cells (3×10^5 cells per well in a 12-well plate) were exposed to BaP with or without FA for 24 h. The supernatant of the culture medium from the various treatments was then collected and levels of IL-1 β and IL-6 were measured using the ELISA kits according to manufacturers' instructions.

2.11. Statistical analysis

Data were presented as mean \pm SD. Statistical analysis was performed using ANOVA or Student's *t* test when appropriate. Significance was defined as $p < 0.05$. All experiments were repeated at least three times.

3. Results

3.1. Cytotoxicity of FA and BaP in microglia BV2 cells

Possible cytotoxic effects of FA and BaP on BV2 cells were determined by measuring the cell viability using the CCK-8 assay. As shown in Fig. 1B and 1C, the viability of BV2 cells was not significantly affected by treatment with FA (2.5, 5, 10, 20, 40, or 80 mg/ml) or BaP (0.01–50 μ M) compared to DMSO-treated controls. Additionally, BaP (10 μ M) pretreatment for 1 h followed by FA treatment (2.5, 5, 10, 20, 40, or 80 mg/ml) for another 24 h also did not significantly affect BV2 cell viability (Fig. 1D). These results indicated that FA and BaP did not induce significant cytotoxicity in BV2 cells, at least with the doses used in this study for the 24 h period. Therefore, in most of the following experiments, BaP at 10 μ M and FA at no higher than 80 mg/ml were used.

3.2. FA protects against BaP-induced DNA damage in BV2 cells

As a classical genotoxic agent, we first assessed the extent of DNA damage in BV2 cells caused by BaP exposure using the comet assay. No comet tail was observed in untreated BV2 (Fig. 2A). In contrast, bright comets of fragmented DNA were detected in BaP-treated BV2, with mean% of total DNA in the tail and olive moment being significantly increased in a dose-dependent manner (Fig. 2A). Interestingly, DNA fragmentation was significantly diminished when FA was added to BV2 after stimulation with BaP for 1 h, indicating that FA could protect BV2 cells from BaP-induced DNA damage (Fig. 2B).

3.3. FA attenuates BaP-induced expression of NO, iNOS, and COX-2 in BV2 cells

Treatment of BV2 cells with BaP significantly increased the generation of NO compared to the controls. On the other hand, treatment of cells with FA significantly attenuated BaP-induced generation of NO

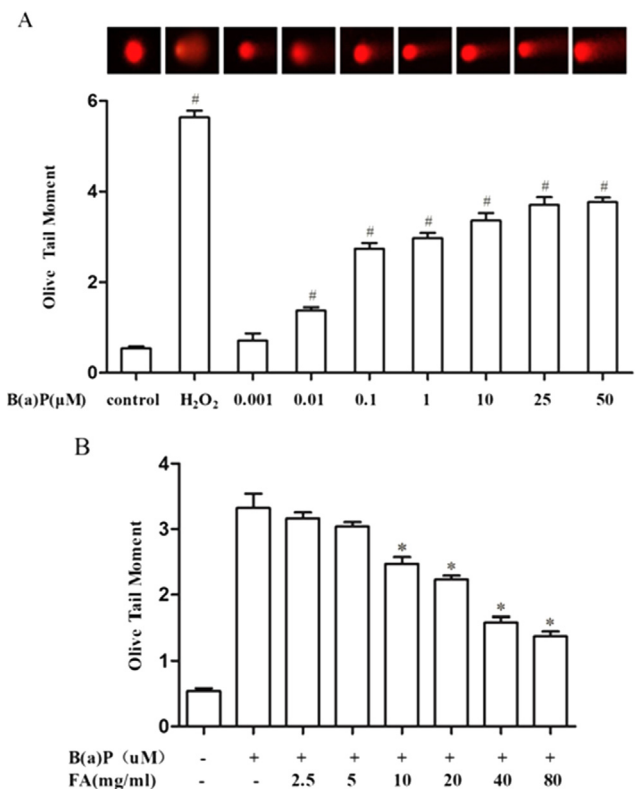


Fig. 2. FA protects BV2 cells from BaP-induced DNA damage. BV2 cells were treated with BaP (0.001–50 μ M) for 6 h (A), or first with BaP (10 μ M) for 1 h followed by FA (2.5, 5, 10, 20, 40, and 80 mg/ml) for 12 h (B). DNA damage was assessed by single-cell electrophoresis (comet assay). Hydrogen peroxide (H₂O₂, 50 mM) was used as positive control. Data are shown as mean \pm SD of at least 100 cells counted on duplicate slides. #P < 0.05, compared to control group; *P < 0.05, compared to BaP-treatment alone.

(Fig. 3A). Similarly, while treatment of BV2 cells with BaP resulted in significantly elevated expression of iNOS, an enzyme responsible for the production of NO, FA treatment significantly decreased BaP-induced expression of iNOS (Fig. 3B and C). The expression levels of COX-2 enzyme, which is responsible for the production of PGE₂, were also examined. As shown in Fig. 3B and D, increased expression of COX-2 by BaP exposure was significantly attenuated by FA.

3.4. FA inhibits BaP-induced ROS generation and lipid peroxidation in BV2 cells

ROS has been implicated in many of the effects of BaP, and therefore, we measured the generation of ROS by BaP exposure. As shown in Fig. 4A, BaP (10 μ M) readily increased intracellular level of ROS in BV2 cells. Nonetheless, FA could inhibit BaP-induced ROS generation in a dose-dependent manner (Fig. 4A). One of the consequences of oxidative stress is lipid peroxidation, which can be reflected by cellular level of MDA. Indeed, our results showed that BaP exposure increased cellular level of MDA, while FA could inhibit such effect (Fig. 4B).

3.5. FA attenuates BaP-induced cytokine production in BV2 cells

The possible inhibitory effects of FA on the production of pro-inflammatory cytokines stimulated by BaP exposure were evaluated. Stimulation of BV2 cells with BaP significantly increased the production of cytokines, such as IL-6 and IL-1 β (Fig. 5A and B). However, when FA was added to the cells, levels of both cytokines were significantly reduced in a dose-dependent manner (Fig. 5A and B), indicating that FA could inhibit the pro-inflammatory response induced by BaP.

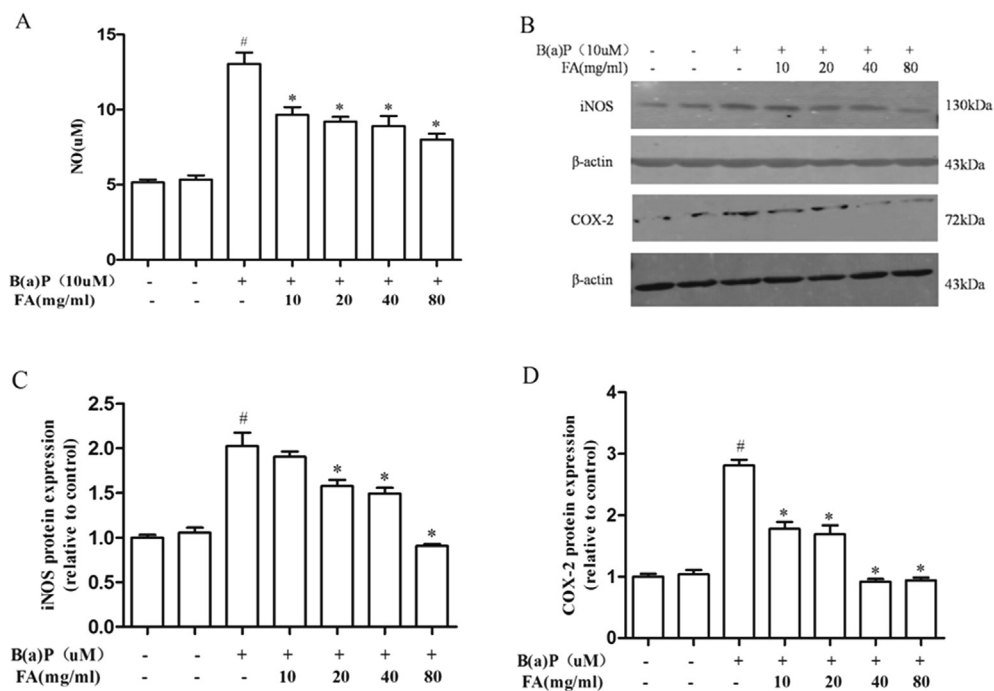


Fig. 3. FA attenuates BaP-induced expression of NO, iNOS, and COX-2 in BV2 cells. BV2 cells were treated with BaP (10 μ M) alone for 24 h, or BaP treatment for 1 h followed by FA (10, 20, 40, and 80 mg/mL) for 24 h (with BaP still in the medium). (A) Generation of NO in culture supernatants was determined using the Griess reagent. (B) Protein expression of iNOS and COX-2 was examined by Western blot analysis. Corresponding densitometry data were shown in (C) and (D). Data were presented as the mean \pm SD of three independent experiments. #P < 0.05, compared to control group; *P < 0.05, compared to BaP-treatment alone.

3.6. FA attenuates BaP-induced activation of NLRP3 inflammasome in BV2 cells

Previous studies have reported that the production of IL-1 β in microglia is mediated by the activation of NLRP3 inflammasome complex, which then induces the cleavage of procaspase-1 in the presence of ASC, one of the components of NLRP3 inflammasome [41]. In accordance with these findings, the results of our RT-PCR and Western blot analysis showed that BaP induced the mRNA and protein expression levels of NLRP3 (Fig. 6A–C). The protein expression of active caspase-1 was also markedly increased in response to BaP stimulation (Fig. 6B and D). However, treatment with FA significantly reduced BaP-induced expression of NLRP3 and the active form of caspase-1 (Fig. 6B–D). The expression of pro-IL-1 β and IL-1 β also exhibited the same pattern (Fig. 6B, E, and F).

4. Discussion

As a potent phenolic antioxidant [42,43], many studies have demonstrated the protective effect of FA against DNA damage induced by various stimuli including chemicals and radiation in different cell or animal models [44–48]. For example, Maurya et al showed that FA protected plasmid DNA from irradiation *in vitro*, as well as peripheral blood leukocytes and bone marrow cells *in vivo* when FA was administered 1 h prior to 4 Gy gamma-radiation exposure. It can also

enhance the DNA repair process in the peripheral blood leukocytes of mice *in vivo* [49]. Sudheer et al also found that FA exerts protective effect against nicotine toxicity both *in vitro* and *in vivo* [50,51]. However, the effects of FA on chemical-induced DNA damage in microglial cells had not been reported, and thus, in the present study, we conducted experiments to examine the effect of FA on BaP-induced DNA damage in BV2 microglial cells. In consistent with previous reports, it was found that FA could also protect BV2 cells against BaP-induced DNA damage in a dose-dependent manner (Fig. 2), which was likely mediated by the regulation of ROS levels (Fig. 4).

In agreement with its genotoxic effect, BaP also exerts neurotoxicity, probably through the induction of many pro-inflammatory factors including cytokines, NO, PGE2, etc. Since microglia is regarded as a major player in the immune response of CNS, we then evaluated the response of BV2 cells after exposure to BaP. Indeed, it was shown that BaP induced the generation of IL-1 β , IL-6, NO, as well as increased expression of iNOS and COX-2 in BV2 cells (Figs. 3 and 5), indicating that microglia activation is involved in the neurotoxicity of BaP. This observation is similar to a report by Dutta et al, in which they had shown that BaP can activate microglia and eventually lead to neuronal death in mouse [52]. On the other hand, we also demonstrated that FA could counteract BaP-induced inflammation response in BV2 cells, thus exerting its potential neuroprotective effect.

Accumulating evidences have shown that the NLRP3 inflammasome is involved in the progression of neurodegenerative diseases such as PD

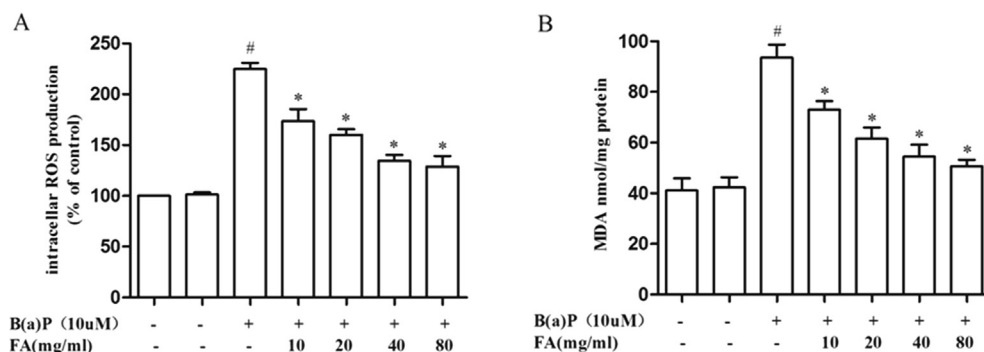


Fig. 4. FA inhibits BaP-induced ROS generation and lipid peroxidation in BV2 cells. BV2 cells were treated with BaP (10 μ M) alone, or with further FA (10, 20, 40, 80 mg/mL) incubation. Intracellular levels of ROS (A) and MDA (B) were measured 12 h later. #P < 0.05, compared to control group; *P < 0.05, compared to BaP-treatment alone.

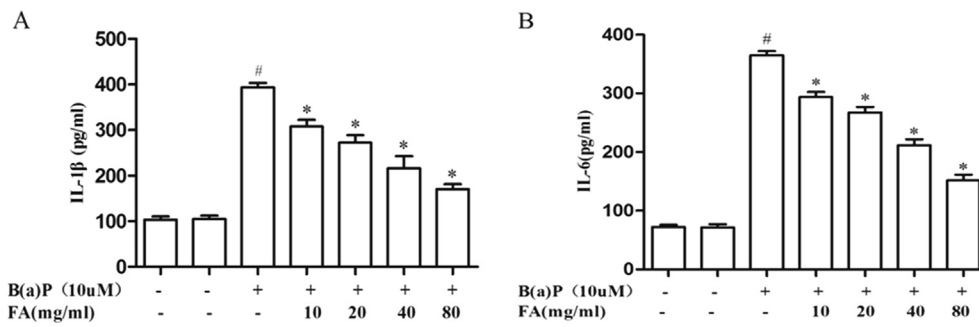


Fig. 5. Inhibitory effect of FA on BaP-induced production of pro-inflammatory cytokines. BV2 cells were incubated with BaP (10 μM) for 24 h, or BaP for 1 h followed by FA treatment (10, 20, 40, or 80 mg/mL) for 24 h (with BaP still in the medium), release of the proinflammatory cytokines, IL-1β (A) and IL-6 (B), into the supernatants was examined by ELISA method. Data were presented as mean ± SD. #P < 0.05, compared to control group; *P < 0.05, compared to BaP-treatment alone.

[53–55]. NLRP3 was originally hypothesized as a cytosolic receptor, which could be activated by a broad range of stimuli. ROS can be induced by many known activators of the NLRP3 inflammasome, and it has been considered as a critical mechanism for triggering NLRP3 inflammasome formation and activation [56,57]. NLRP3 protein levels have been shown to be a limiting step in inflammasome activation [58,59]. Although BaP is known to induce ROS generation, however, to date there had been no report showing the direct activation of NLRP3 inflammasome. In this study, we found that BaP could increase the expression of NLRP3 at both mRNA and protein levels in BV2 cells,

providing the first piece of evidence for the activation of NLRP3 inflammasome by BaP (Fig. 6).

Two signals are required for NLRP3 inflammasome-mediated IL-1β production. The first signal induces the activation of nuclear transcription factor-κB (NF-κB), which in turn leads to increased expression of NLRP3 and pro-IL-1β, a prerequisite for inflammasome activation. The second signal then directly activates the NLRP3 inflammasome to induce the cleavage of caspase-1, which is responsible for the maturation of IL-1β. On the other hand, it has been shown that FA can interfere with the activation of NLRP3 inflammasome. For instance, FA can

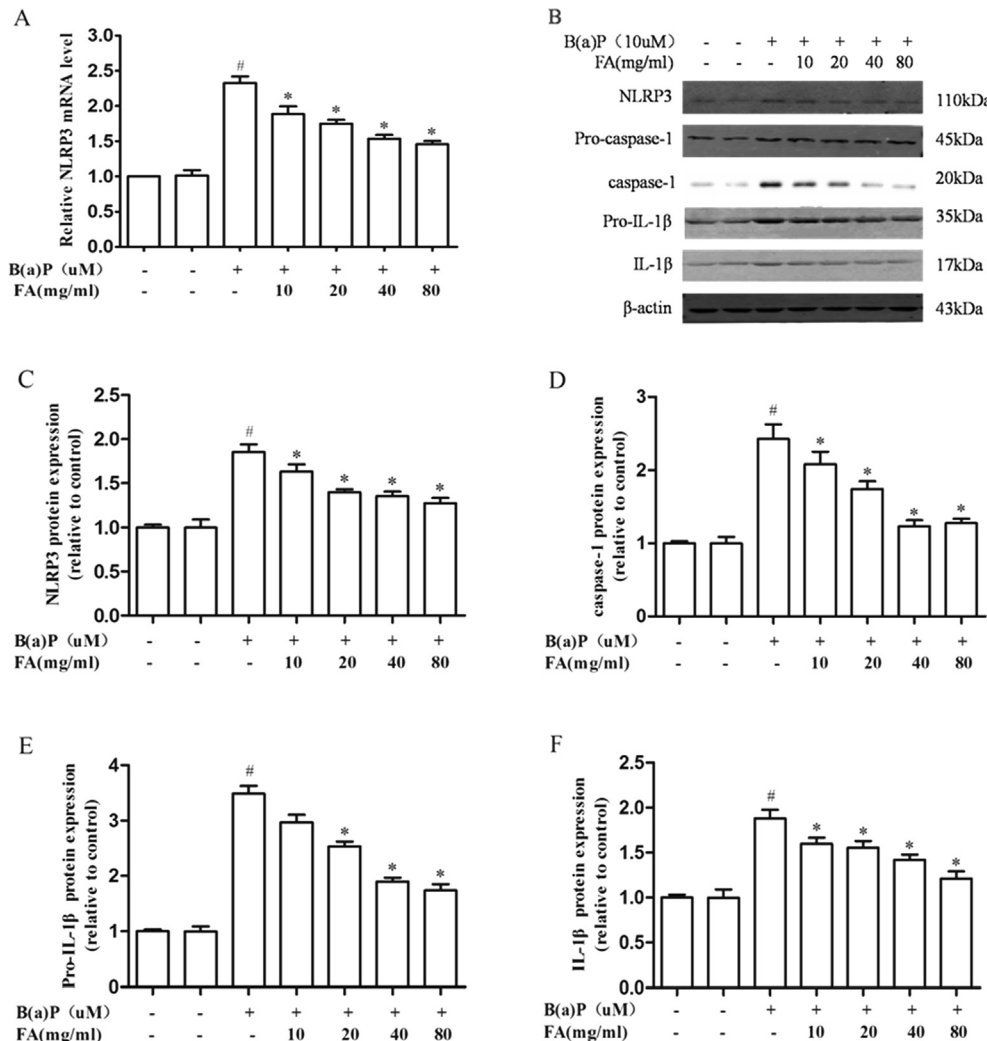


Fig. 6. FA inhibits BaP-induced NLRP3 inflammasome activation in BV2 microglia. BV2 cells were incubated with BaP (10 μM) alone, or BaP for 1 h followed by FA treatment (10, 20, 40, and 80 mg/mL) for 24 h, mRNA level of NLRP3 was measured by RT-PCR, (A), protein expression levels of NLRP3, pro-IL-1β, pro-caspase-1, cleaved caspase-1, and IL-1β in cell lysates were measured by Western blot and densitometry analysis (B-F). The data were generated from three independent experiments. Data were presented as mean ± SD. #P < 0.05, compared to control group; *P < 0.05, compared to BaP-treatment alone.

suppress monosodium urate crystal-induced inflammation, including NLRP3 mRNA expression in rats [60]. Also, FA can inhibit NLRP3 inflammasome activation in mice under chronic unpredictable mild stress [61]. In order to determine the effect of FA on BaP-induced NLRP3 inflammasome activation, we examined the expression of the several key components during NLRP3 inflammasome activation. It was found that FA reduced the expression of NLRP3 and pro-IL-1 β in BV2 microglia, and suppressed the activation of caspase-1 and the maturation of IL-1 β induced by BaP (Fig. 6). Thus, our data further confirmed the anti-inflammatory function of FA.

In a recent study, Rehman et al reported that FA can also rescue lipopolysaccharide (LPS)-induced neurotoxicity via regulating the Toll-like receptor 4 (TLR4) in mouse hippocampus [62]. They have shown that FA can directly target TLR4, thus inhibiting the activation of glial cells, as well as the down-stream signaling molecules, including iNOS, COX2, TNF- α , and IL-1 β . These observations are in agreement with our results, suggesting that the inflammatory response might be a shared common feature for cellular response to environmental stimuli, regardless of chemical or biological factors. However, they focused on the NF- κ B and JNK pathways instead of the NLRP3 pathway.

In conclusion, in the present study, we have shown that the environmental genotoxin BaP could activate microglia cells and induce ROS generation, which was accompanied by the activation of NLRP3 inflammasome, as well as the production of many pro-inflammatory factors. In contrast, FA inhibited the toxic effects of BaP, and the ROS and NLRP3 inflammasome might be its targets. Taken together, our data suggest that FA could protect cells against oxidative stress and cytotoxicity caused by certain chemicals, and may be even beneficial in the treatment of neurodegenerative diseases.

Acknowledgement

This work was supported in part by grants from the Program for Humanistic and Social Science of the Education Department of Hubei Province (15Q226) to Y. Bao; Program for Discipline Construction of Pharmacy (2018-19XZY01); Science and Technology Research Program of Xianning (XNKJ-1811); and Leading Disciplines of Clinical Medicine of Hubei University of Science and Technology (LCZX201512) to S. Shan; the Key Research Program of Zhejiang Provincial Natural Science Foundation (LZ19H260001) and National Science Foundation of China (31971138) to J. Yang.

Declaration of Competing Interest

All authors declare that they have no conflict of interest.

Appendix A. Supplementary material

Supplementary data to this article can be found online at <https://doi.org/10.1016/j.intimp.2019.105980>.

References

- [1] U.K. Hanisch, Microglia as a source and target of cytokines, *Glia* 40 (2002) 140–155, <https://doi.org/10.1002/glia.10161>.
- [2] L. Minghetti, G. Levi, Microglia as effector cells in brain damage and repair: focus on prostanooids and nitric oxide, *Prog. Neurobiol.* 54 (1998) 99–125, [https://doi.org/10.1016/S0304-0082\(97\)00052-X](https://doi.org/10.1016/S0304-0082(97)00052-X).
- [3] C. D'Mello, M.G. Swain, Immune-to-brain communication pathways in inflammation-associated sickness and depression, *Curr. Top. Behav. Neurosci.* 31 (2017) 73–94, https://doi.org/10.1007/7854_2016_37.
- [4] R. Dantzer, J.C. O'Connor, G.G. Freund, R.W. Johnson, K.W. Kelley, From inflammation to sickness and depression: when the immune system subjugates the brain, *Nat. Rev. Neurosci.* 9 (2008) 46–56, <https://doi.org/10.1038/nrn2297>.
- [5] T. Pollmacher, M. Haack, A. Schulz, A. Reichenberg, R. Yirmiya, Low levels of circulating inflammatory cytokines—do they affect human brain functions? *Brain Behav. Immun.* 16 (2002) 525–532, [https://doi.org/10.1016/S0889-1591\(02\)00004-1](https://doi.org/10.1016/S0889-1591(02)00004-1).
- [6] M.L. Block, J.S. Hong, Microglia and inflammation-mediated neurodegeneration: multiple triggers with a common mechanism, *Prog. Neurobiol.* 76 (2005) 77–98, <https://doi.org/10.1016/j.pneurobio.2005.06.004>.
- [7] L.E. Rojo, J.A. Fernandez, A.A. Maccioni, J.M. Jimenez, R.B. Maccioni, Neuroinflammation: implications for the pathogenesis and molecular diagnosis of Alzheimer's disease, *Arch. Med. Res.* 39 (2008) 1–16, <https://doi.org/10.1016/j.arcmed.2007.10.001>.
- [8] F. Zipp, O. Aktas, The brain as a target of inflammation: common pathways link inflammatory and neurodegenerative diseases, *Trends Neurosci.* 29 (2006) 518–527, <https://doi.org/10.1016/j.tins.2006.07.006>.
- [9] A. Pisanu, D. Lecca, G. Mulas, J. Wardas, G. Simbula, S. Spiga, A.R. Carta, Dynamic changes in pro- and anti-inflammatory cytokines in microglia after PPAR-gamma agonist neuroprotective treatment in the MPTP mouse model of progressive Parkinson's disease, *Neurobiol. Dis.* 71 (2014) 280–291, <https://doi.org/10.1016/j.nbd.2014.08.011>.
- [10] E. Oh, E. Lee, H. Im, H.S. Kang, W.W. Jung, N.H. Won, E.M. Kim, D. Sul, Evaluation of immuno- and reproductive toxicities and association between immunotoxicological and genotoxicological parameters in waste incineration workers, *Toxicology* 210 (2005) 65–80, <https://doi.org/10.1016/j.tox.2005.01.008>.
- [11] M. Das, P.K. Seth, H. Mukhtar, Distribution of benzo(a)pyrene in discrete regions of rat brain, *Bull. Environ. Contam. Toxicol.* 35 (1985) 500–504.
- [12] A. Ramesh, F. Inyang, D.B. Hood, A.E. Archibong, M.E. Knuckles, A.M. Nyanda, Metabolism, bioavailability, and toxicokinetics of benzo(alpha)pyrene in F-344 rats following oral administration, *Exp. Toxicol. Pathol.* 53 (2001) 275–290.
- [13] P. Stephanou, M. Konstandi, P. Pappas, M. Marselos, Alterations in central monoaminergic neurotransmission induced by polycyclic aromatic hydrocarbons in rats, *Eur. J. Drug Metab. Pharmacokinet* 23 (1998) 475–481, <https://doi.org/10.1007/BF03189998>.
- [14] C. Chen, Y. Tang, X. Jiang, Y. Qi, S. Cheng, C. Qiu, B. Peng, B. Tu, Early postnatal benzo(a)pyrene exposure in Sprague-Dawley rats causes persistent neurobehavioral impairments that emerge postnatally and continue into adolescence and adulthood, *Toxicol. Sci.* 125 (2012) 248–261, <https://doi.org/10.1093/toxsci/kfr265>.
- [15] C. Li, J. Wang, Q. Su, K. Yang, C. Chen, X. Jiang, T. Han, S. Cheng, T. Mo, R. Zhang, B. Peng, Y. Guo, P.N. Baker, B. Tu, Y. Xia, Postnatal subacute benzo(a)pyrene exposure caused neurobehavioral impairment and metabolomic changes of cerebellum in the early adulthood period of Sprague-Dawley rats, *Neurotox. Res.* 33 (2018) 812–823, <https://doi.org/10.1007/s12640-017-9832-8>.
- [16] Q. Niu, H. Zhang, X. Li, M. Li, Benzo(a)pyrene-induced neurobehavioral function and neurotransmitter alterations in coke oven workers, *Occup. Environ. Med.* 67 (2010) 444–448, <https://doi.org/10.1136/oem.2009.047969>.
- [17] C.R. Saunders, D.C. Shockley, M.E. Knuckles, Behavioral effects induced by acute exposure to benzo(a)pyrene in F-344 rats, *Neurotox. Res.* 3 (2001) 557–579.
- [18] I.A. Adedara, O. Owoeye, M.A. Aiyegbusi, J.O. Dagunduro, Y.M. Daramola, E.O. Farombi, Kolaviron protects against benzo(a)pyrene-induced functional alterations along the brain-pituitary-gonadal axis in male rats, *Environ. Toxicol. Pharmacol.* 40 (2015) 459–470, <https://doi.org/10.1016/j.etap.2015.07.015>.
- [19] L. Smerdova, J. Neca, J. Svobodova, J. Topinka, J. Schmuczerova, A. Kozubik, M. Machala, J. Vondracek, Inflammatory mediators accelerate metabolism of benzo(a)pyrene in rat alveolar type II cells: the role of enhanced cytochrome P450 1B1 expression, *Toxicology* 314 (2013) 30–38, <https://doi.org/10.1016/j.tox.2013.09.001>.
- [20] S.J. Zheng, H.J. Tian, J. Cao, Y.Q. Gao, Exposure to di(n-butyl)phthalate and benzo(a)pyrene alters IL-1 β secretion and subset expression of testicular macrophages, resulting in decreased testosterone production in rats, *Toxicol. Appl. Pharmacol.* 248 (2010) 28–37, <https://doi.org/10.1016/j.taap.2010.07.008>.
- [21] L. Umannova, M. Machala, J. Topinka, J. Schmuczerova, P. Krcmar, J. Neca, K. Stujanova, A. Kozubik, J. Vondracek, Benzo(a)pyrene and tumor necrosis factor- α coordinately increase genotoxic damage and the production of proinflammatory mediators in alveolar epithelial type II cells, *Toxicol. Lett.* 206 (2011) 121–129, <https://doi.org/10.1016/j.toxlet.2011.06.029>.
- [22] H.V. Gelboin, Benzo(alpha)pyrene metabolism, activation and carcinogenesis: role and regulation of mixed-function oxidases and related enzymes, *Physiol. Rev.* 60 (1980) 1107–1166.
- [23] K.B. Kim, B.M. Lee, Oxidative stress to DNA, protein, and antioxidant enzymes (superoxide dismutase and catalase) in rats treated with benzo(a)pyrene, *Cancer Lett.* 113 (1997) 205–212, [https://doi.org/10.1016/S0304-3835\(97\)04610-7](https://doi.org/10.1016/S0304-3835(97)04610-7).
- [24] F. Omodeo-Sale, L. Cortelezzi, Z. Vommaro, D. Scaccabarozzi, A.M. Dondorp, Dysregulation of L-arginine metabolism and bioavailability associated to free plasma heme, *Am. J. Physiol. Cell Physiol.* 299 (2010) C148–154, <https://doi.org/10.1152/ajpcell.00405.2009>.
- [25] Y. Zhang, V. Brovkovich, F. Tan, B.S. Lee, T. Sharma, R.A. Skidgel, Dynamic receptor-dependent activation of inducible nitric-oxide synthase by ERK-mediated phosphorylation of Ser745, *J. Biol. Chem.* 282 (2007) 32453–32461, <https://doi.org/10.1074/jbc.M706242200>.
- [26] J.U. Johansson, N.S. Woodling, Q. Wang, M. Panchal, X. Liang, A. Trueba-Saiz, H.D. Brown, S.D. Mhatre, T. Loui, K.I. Andreasson, Prostaglandin signaling suppresses beneficial microglial function in Alzheimer's disease models, *J. Clin. Invest.* 125 (2015) 350–364, <https://doi.org/10.1172/JCI77487>.
- [27] L.W. Fan, A. Kaizaki, L.T. Tien, Y. Pang, S. Tanaka, S. Numazawa, A.J. Bhatt, Z. Cai, Celecoxib attenuates systemic lipopolysaccharide-induced brain inflammation and white matter injury in the neonatal rats, *Neuroscience* 240 (2013) 27–38, <https://doi.org/10.1016/j.neuroscience.2013.02.041>.
- [28] Q. Xia, Q. Hu, H. Wang, H. Yang, F. Gao, H. Ren, D. Chen, C. Fu, L. Zheng, X. Zhen, Z. Ying, G. Wang, Induction of COX-2-PGE2 synthesis by activation of the MAPK/ERK pathway contributes to neuronal death triggered by TDP-43-depleted microglia, *Cell Death. Dis.* 6 (2015) e1702, <https://doi.org/10.1038/cddis.2015.69>.
- [29] L. Franchi, R. Munoz-Planillo, G. Nunez, Sensing and reacting to microbes through

- the inflammasomes, *Nat. Immunol.* 13 (2012) 325–332, <https://doi.org/10.1038/ni.2231>.
- [30] C. Conforti-Andreoni, P. Ricciardi-Castagnoli, A. Mortellaro, The inflammasomes in health and disease: from genetics to molecular mechanisms of autoinflammation and beyond, *Cell Mol. Immunol.* 8 (2011) 135–145, <https://doi.org/10.1038/cmi.2010.81>.
- [31] Y. Jin, E.Z. Yan, X.M. Li, Y. Fan, Y.J. Zhao, Z. Liu, W.Z. Liu, Neuroprotective effect of sodium ferulate and signal transduction mechanisms in the aged rat hippocampus, *Acta Pharmacol. Sin.* 29 (2008) 1399–1408, <https://doi.org/10.1111/j.1745-7254.2008.00848.x>.
- [32] J. Kanski, M. Aksenova, A. Stoyanova, D.A. Butterfield, Ferulic acid antioxidant protection against hydroxyl and peroxy radical oxidation in synaptosomal and neuronal cell culture systems in vitro: structure-activity studies, *J. Nutr. Biochem.* 13 (2002) 273–281, [https://doi.org/10.1016/S0955-2863\(01\)00215-7](https://doi.org/10.1016/S0955-2863(01)00215-7).
- [33] B.W. Kim, S. Koppula, S.Y. Park, Y.S. Kim, P.J. Park, J.H. Lim, I.S. Kim, D.K. Choi, Attenuation of neuroinflammatory responses and behavioral deficits by Ligusticum officinale (Makino) Kitag in stimulated microglia and MPTP-induced mouse model of Parkinson's disease, *J. Ethnopharmacol.* 164 (2015) 388–397, <https://doi.org/10.1016/j.jep.2014.11.004>.
- [34] P. Picone, M.L. Bondi, G. Montana, A. Bruno, G. Pitarresi, G. Giammona, M. Di Carlo, Ferulic acid inhibits oxidative stress and cell death induced by Ab oligomers: improved delivery by solid lipid nanoparticles, *Free Radic. Res.* 43 (2009) 1133–1145.
- [35] T. Yabe, H. Hirahara, N. Harada, N. Ito, T. Nagai, T. Sanagi, H. Yamada, Ferulic acid induces neural progenitor cell proliferation in vitro and in vivo, *Neuroscience* 165 (2010) 515–524, <https://doi.org/10.1016/j.neuroscience.2009.10.023>.
- [36] P.O. Koh, Ferulic acid prevents cerebral ischemic injury-induced reduction of hippocampal expression, *Synapse* 67 (2013) 390–398, <https://doi.org/10.1002/syn.21649>.
- [37] T. Mori, N. Koyama, M.V. Guillot-Sestier, J. Tan, T. Town, Ferulic acid is a nutraceutical beta-secretase modulator that improves behavioral impairment and alzheimer-like pathology in transgenic mice, *PLoS. One* 8 (2013) e55774, <https://doi.org/10.1371/journal.pone.0055774>.
- [38] R. Sultana, A. Ravagna, H. Mohammad-Abdul, V. Calabrese, D.A. Butterfield, Ferulic acid ethyl ester protects neurons against amyloid beta-peptide(1–42)-induced oxidative stress and neurotoxicity: relationship to antioxidant activity, *J. Neurochem.* 92 (2005) 749–758, <https://doi.org/10.1111/j.1471-4159.2004.02899.x>.
- [39] W.K. Jung, D.Y. Lee, C. Park, Y.H. Choi, I. Choi, S.G. Park, S.K. Seo, S.W. Lee, S.S. Yea, S.C. Ahn, C.M. Lee, W.S. Park, J.H. Ko, I.W. Choi, Cilostazol is anti-inflammatory in BV2 microglial cells by inactivating nuclear factor-kappaB and inhibiting mitogen-activated protein kinases, *Br. J. Pharmacol.* 159 (2010) 1274–1285, <https://doi.org/10.1111/j.1476-5381.2009.00615.x>.
- [40] Y. Yu, W. Zhu, H. Diao, C. Zhou, F.F. Chen, J. Yang, A comparative study of using comet assay and gammaH2AX foci formation in the detection of N-methyl-N'-nitro-N-nitrosoguanidine-induced DNA damage, *Toxicol. In Vitro* 20 (2006) 959–965, <https://doi.org/10.1016/j.tiv.2006.01.004>.
- [41] C.M. Lee, D.S. Lee, W.K. Jung, J.S. Yoo, M.J. Yim, Y.H. Choi, S. Park, S.K. Seo, J.S. Choi, Y.M. Lee, W.S. Park, I.W. Choi, Benzyl isothiocyanate inhibits inflammasome activation in E. coli LPS-stimulated BV2 cells, *Int. J. Mol. Med.* 38 (2016) 912–918, <https://doi.org/10.3892/ijmm.2016.2667>.
- [42] T. Eitsuka, N. Tatewaki, H. Nishida, T. Kurata, K. Nakagawa, T. Miyazawa, Synergistic inhibition of cancer cell proliferation with a combination of delta-tocotrienol and ferulic acid, *Biochem. Biophys. Res. Commun.* 453 (2014) 606–611, <https://doi.org/10.1016/j.bbrc.2014.09.126>.
- [43] C. Mancuso, R. Santangelo, Ferulic acid: pharmacological and toxicological aspects, *Food Chem. Toxicol.* 65 (2014) 185–195, <https://doi.org/10.1016/j.fct.2013.12.024>.
- [44] S. Catino, F. Paciello, F. Miceli, R. Rolesi, D. Troiani, V. Calabrese, R. Santangelo, C. Mancuso, Ferulic acid regulates the Nrf2/heme oxygenase-1 system and counteracts trimethyltin-induced neuronal damage in the human neuroblastoma cell line SH-SY5Y, *Front. Pharmacol.* 6 (2015) 305, <https://doi.org/10.3389/fphar.2015.00305>.
- [45] U. Das, K. Manna, A. Khan, M. Sinha, S. Biswas, A. Sengupta, A. Chakraborty, S. Day, Ferulic acid (FA) abrogates gamma-radiation induced oxidative stress and DNA damage by up-regulating nuclear translocation of Nrf2 and activation of NHEJ pathway, *Free Radic. Res.* 51 (2017) 47–63, <https://doi.org/10.1080/10715762.2016.1267345>.
- [46] D.K. Maurya, T.P. Devasagayam, Ferulic acid inhibits gamma radiation-induced DNA strand breaks and enhances the survival of mice, *Cancer Biother. Radiopharm.* 28 (2013) 51–57, <https://doi.org/10.1089/cbr.2012.1263>.
- [47] B.C. Scott, J. Butler, B. Halliwell, O.I. Aruoma, Evaluation of the antioxidant actions of ferulic acid and catechins, *Free Radic. Res. Commun.* 19 (1993) 241–253.
- [48] A.R. Sudheer, S. Muthukumar, N. Devipriya, H. Devaraj, V.P. Menon, Influence of ferulic acid on nicotine-induced lipid peroxidation, DNA damage and inflammation in experimental rats as compared to N-acetylcysteine, *Toxicology* 243 (2008) 317–329, <https://doi.org/10.1016/j.tox.2007.10.016>.
- [49] N.R. Prasad, M. Srinivasan, K.V. Pugalendi, V.P. Menon, Protective effect of ferulic acid on gamma-radiation-induced micronuclei, dicentric aberration and lipid peroxidation in human lymphocytes, *Mutat. Res.* 603 (2006) 129–134, <https://doi.org/10.1016/j.mrgentox.2005.11.002>.
- [50] A.R. Sudheer, K. Chandran, S. Marimuthu, V.P. Menon, Ferulic Acid modulates altered lipid profiles and prooxidant/antioxidant status in circulation during nicotine-induced toxicity: a dose-dependent study, *Toxicol. Mech. Methods* 15 (2005) 375–381, <https://doi.org/10.1080/15376520500194783>.
- [51] A.R. Sudheer, S. Muthukumar, C. Kalpana, M. Srinivasan, V.P. Menon, Protective effect of ferulic acid on nicotine-induced DNA damage and cellular changes in cultured rat peripheral blood lymphocytes: a comparison with N-acetylcysteine, *Toxicol. In Vitro* 21 (2007) 576–585, <https://doi.org/10.1016/j.tiv.2006.11.006>.
- [52] K. Dutta, D. Ghosh, A. Nazmi, K.L. Kumawat, A. Basu, A common carcinogen benzo[a]pyrene causes neuronal death in mouse via microglial activation, *PLoS One* 5 (2010) e9984, <https://doi.org/10.1371/journal.pone.0009984>.
- [53] Z. Fan, M. Lu, C. Qiao, Y. Zhou, J.H. Ding, G. Hu, MicroRNA-7 enhances subventricular zone neurogenesis by inhibiting NLRP3/caspase-1 axis in adult neural stem cells, *Mol. Neurobiol.* 53 (2016) 7057–7069, <https://doi.org/10.1007/s12035-015-9620-5>.
- [54] C. Qiao, L.X. Zhang, X.Y. Sun, J.H. Ding, M. Lu, G. Hu, Deficiency Alleviates Dopaminergic Neuronal Death via Inhibiting Caspase-7/AIF Pathway in MPTP/p Mouse Model of Parkinson's Disease, *Mol. Neurobiol.* 54 (2017) 4292–4302, <https://doi.org/10.1007/s12035-016-9980-5>.
- [55] Y. Zhou, M. Lu, R.H. Du, C. Qiao, C.Y. Jiang, K.Z. Zhang, J.H. Ding, G. Hu, MicroRNA-7 targets Nod-like receptor protein 3 inflammasome to modulate neuroinflammation in the pathogenesis of Parkinson's disease, *Mol. Neurodegener.* 11 (2016) 28, <https://doi.org/10.1186/s13024-016-0094-3>.
- [56] J.M. Abais, M. Xia, Y. Zhang, K.M. Boini, P.L. Li, Redox regulation of NLRP3 inflammasomes: ROS as trigger or effector? *Antioxid. Redox. Signal.* 22 (2015) 1111–1129, <https://doi.org/10.1089/ars.2014.5994>.
- [57] J. Tschopp, K. Schroder, NLRP3 inflammasome activation: The convergence of multiple signalling pathways on ROS production? *Nat. Rev. Immunol.* 10 (2010) 210–215, <https://doi.org/10.1038/nri2725>.
- [58] F.G. Bauernfeind, G. Horvath, A. Stutz, E.S. Alnemri, K. MacDonald, D. Speert, T. Fernandes-Alnemri, J. Wu, B.G. Monks, K.A. Fitzgerald, V. Hornung, E. Latz, Cutting edge: NF-kappaB activating pattern recognition and cytokine receptors license NLRP3 inflammasome activation by regulating NLRP3 expression, *J. Immunol.* 183 (2009) 787–791, <https://doi.org/10.4049/jimmunol.0901363>.
- [59] L. Franchi, T. Eigenbrod, G. Nunez, Cutting edge: TNF-alpha mediates sensitization to ATP and silica via the NLRP3 inflammasome in the absence of microbial stimulation, *J. Immunol.* 183 (2009) 792–796, <https://doi.org/10.4049/jimmunol.0900173>.
- [60] H.M. Doss, C. Dey, C. Sudandiradoss, M.K. Rasool, Targeting inflammatory mediators with ferulic acid, a dietary polyphenol, for the suppression of monosodium urate crystal-induced inflammation in rats, *Life Sci.* 148 (2016) 201–210, <https://doi.org/10.1016/j.lfs.2016.02.004>.
- [61] Y.M. Liu, J.D. Shen, L.P. Xu, H.B. Li, Y.C. Li, L.T. Yi, Ferulic acid inhibits neuroinflammation in mice exposed to chronic unpredictable mild stress, *Int. Immunopharmacol.* 45 (2017) 128–134, <https://doi.org/10.1016/j.intimp.2017.02.007>.
- [62] S.U. Rehman, T. Ali, S.I. Alam, R. Ullah, A. Zeb, K.W. Lee, B.P.F. Rutten, M.O. Kim, Ferulic acid rescues LPS-induced neurotoxicity via modulation of the TLR4 Receptor in the mouse hippocampus, *Mol. Neurobiol.* 56 (2019) 2774–2790, <https://doi.org/10.1007/s12035-018-1280-9>.